Energy Saving Evaluation of the Ventilated BIPV Walls

Chi-ming Lai [1*] and Yi-pin Lin [2]

[1] *Department of Civil Engineering, National Cheng Kung University, Taiwan*
[2]*Department of Interior Design, Tung Fang Design University, Taiwan*
[*]*1, University Road, Tainan City, 701, Taiwan, cmlai@mail.ncku.edu.tw (Dr. Chi-ming Lai); purple5028@gmail.com (Dr. Yi-pin Lin)*

ABSTRACT

This study integrates photovoltaic (PV) system, building structure, and heat flow mechanism to propose the ventilated building-integrated photovoltaics (BIPV) walls. Energy-saving potential of the ventilated BIPV walls was investigated via engineering considerations and computational fluid dynamics (CFD) simulations. The results show that the heat removal rate and indoor heat gain of the proposed ventilated BIPV walls were dominantly affected by outdoor wind velocity and airflow channel width. Correlations for predicting the heat removal rate and indoor heat gain are introduced. After considering building construction practices, this prototype was transformed into a curtain wall structure that complemented the design of the overall construction.

Keywords: Energy; BIPV; building; computational fluid dynamics; photovoltaic

INTRODUCTION

Building-integrated photovoltaics (BIPV) refers to an architectural design approach that combines photovoltaic (PV) panels with the building construction system. This combination allows BIPV to not only feature a power generation function but also to become part of the building façade. However, solar irradiation, received by PV cell, would be transferred into heat and cause the increase of PV cell the temperature, which is associated with the generation efficiency. Dubey and Tiwari showed that the increase in cell temperature decreases the cell efficiency and at the end of the day it will again increase due to decrease in cell temperature (Dubey and Tiwari, 2009). Therefore, whenever possible, it is necessary to fully enhance a PV's heat dissipation. Because an irradiated PV panel is a heat source in the BIPV construction, a double-skin design concept can possibly be used to design the BIPV structure as a ventilated BIPV.

There is still limited existing literature on ventilated BIPV effectiveness on solar heat removal, and a lack of similar ventilated BIPV structures. This study aims to understand the thermal effect on the innovative BIPV module and to explore the use of thermal management to decrease the thermal impact. An innovative ventilated BIPV wall design is proposed and

evaluated via engineering considerations and computational fluid dynamics (CFD) simulations.

RESEARCH METHODS

Before establishing the physical model, we must first explore a practical method for replacing an existing exterior wall with ventilated BIPV construction. In Taiwan, residential buildings are often composed of reinforced concrete or light steel. A conventional exterior wall structure for a light steel house is shown in Figure 1. In such constructions, the C-shaped or square steel columns are erected to be the main support where outdoor and indoor wall panels are attached.
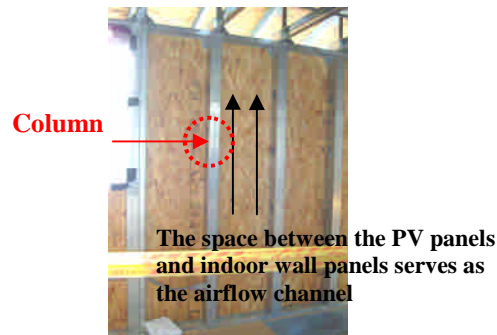
**Figure 1. The exterior wall structure of a light steel house**

As shown in Figure 2, this study suggests the replacement of the exterior wall panels with PV panels, leaving the space between the exterior and interior walls as an airflow channel to provide natural ventilation and heat dissipation for the ventilated BIPV wall.
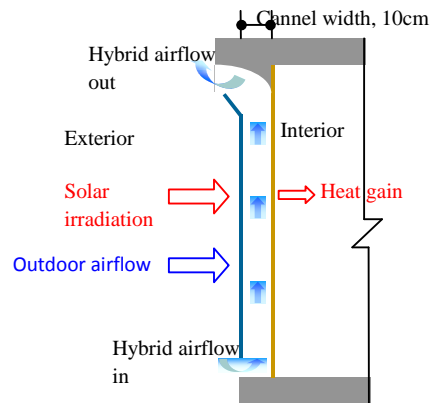
Figure 2. The ventilated BIPV wall proposed in this study

The channel space, which has the same dimensions as the column width, can also be used for installation of PV cables. Each row of PV panels (i.e., every external wall unit divided by two columns) has an air inlet at its base. The outdoor airflow enters through the inlet into the mezzanine channel, which is formed by the PV panels and indoor decorative boards. After flowing through the entire row of PV panels, the airflow in the channel is discharged from the outlet located on top of the PV panels. A detailed design of the outlet vent has been simulated using CFD technology to ensure that the outdoor airflow will not flow in through the top air vent and reduce the strength of the buoyancy.

The investigated model space has the dimensions 6.1 m (L) × 3.2 m (W) × 2.85m (H) and the exterior wall of the house is designed as the ventilated BIPV wall, shown in Figure 3. The main parameters for the model space used for the study are detailed in Table 1 and illustrated in Figure 3.
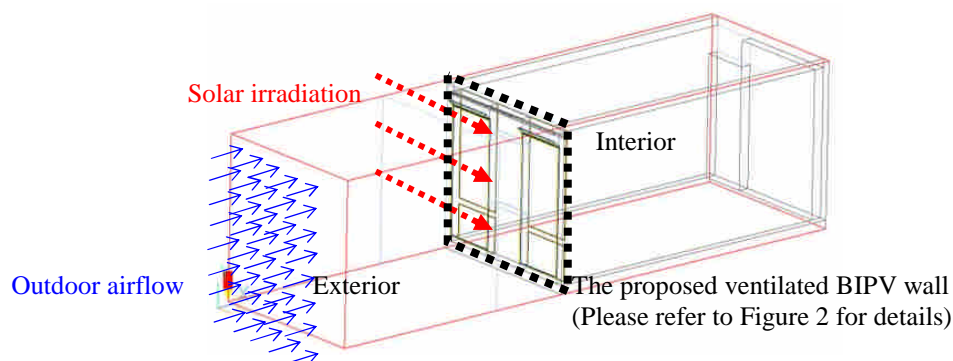
Figure 3. Schematic diagram of the proposed ventilated BIPV and investigated space

Table 1. Main parameters for the CFD simulations

Item		Settings
1. Outdoor environment	(Typical weather conditions in Taiwan)	Fix the outdoor air temperature at 29 ^{o}C Fix the solar irradiation at 600 W/m^2 Change the air velocity Vo (0.5, 1.0, 2.0 m/s)
2. Exterior wall	Original exterior wall location	Replace the original exterior wall with the proposed ventilated BIPV wall
	BIPV airflow channel width	Change the airflow channel width W (5, 10, 15, 20 cm) (Change under the premise of meeting the actual exterior wall structure of the building)
	Indoor vent	Fix the opening area
		Change the opening height H (15, 30, 45, 60, 75, 90 cm) (Under the premise of meeting the actual interior design)
	Thermal properties	PV panel: k=60W/mK; ρ=7854 kg/m3; Cp=434 J/kg K indoor wall panel (wood): k=0.16 W/mK; ρ=720 kg/m3; Cp=1255 J/kg K
3. Indoor space	Indoor furniture	No furnishings
	Indoor heat source	No indoor heat source
4. Indoor partition wall		Close the door (ignore cracks in interior door) Adiabatic wall

Numerical simulations of the physical problem under consideration were performed using a finite volume method to solve the governing equations and boundary conditions mentioned above. A CFD code, PHOENICS, was used to simulate the airflow and temperature distributions. The governing equations solved by PHOENICS include the three-dimensional time-dependent incompressible Navier-Stokes equation, the time-dependent convection diffusion equation and k-ε turbulence equations. These formulated equations can be found in the PHOENICS user's manual (Spalding, 1994) and in any CFD textbook. For the k-ε turbulence equation, the empirical turbulence coefficients were assigned as σ_k=1.0, σ_ε=1.22, $\sigma_{\varepsilon 1}$=1.44, $\sigma_{\varepsilon 2}$=1.92, and Cμ=0.09. These values were widely accepted in the CFD k-ε model. To bridge the steep dependent variable gradients close to the solid surface, the general wall

function was employed. The iterative calculation was continued until a prescribed relative convergence of 10^{-3} was satisfied for all the field variables of this problem. The numerical simulation accuracy depends on the resolution of the computational mesh, and a finer grid leads to more accurate solutions. In this study, a grid system with approximately 52 x 162 x 120 cells was used for the numerical simulation. Increasing the number of cells will provide information that is more accurate. However, increasing the number of cells will also increase the computation resources required.

When sunlight radiates onto the ventilated BIPV wall, thermal energy will be absorbed, causing the temperature of the PV panels to rise and the air in the airflow channel to be heated. These reactions will generate buoyancy to push up the channel air and remove part of the heat via a natural convection mechanism. The other part of the heat energy will be transmitted into the indoor space by means of thermal conduction through the interior wall panels of the BIPV structure. Furthermore, the outdoor air can also flow into the airflow channel of the ventilated BIPV wall through the inlet below the BIPV structure to generate forced convection and remove the heat gain on the PV panels. A mixed convection mechanism is generated within the airflow channel. By measuring the temperature and airflow rate, the amount of the heat transfer rate $\dot{Q}_{ch}$ (W) that has been carried away by convective airflow in the channel can be calculated as shown in equation (1).

$$\dot{Q}_{ch} = \dot{m}C_P(T_{m,o} - T_{m,i}) \tag{1}$$

Where $\dot{m}$ is the mass flow rate (kg/s) of the channel airflow, $\dot{m} = \rho V_{m,o}A_C$, ρ is the air density (kg/m^3), $V_{m,o}$ is the average velocity (m/s) at the outlet of channel airflow, A_c is the cross-sectional area of the channel (m^2), C_p is the air specific heat (J/kg ^{o}C), $T_{m,o}$ is the average air temperature at the outlet, and $T_{m,i}$ is the average air temperature (^{o}C) at the inlet.

Solar radiation penetrates a building's opening directly to heat the indoor air or indoor facilities. It is also able to heat the outdoor air or exterior walls to transmit thermal energy through the building skin. Indoor heat gain is a result of these two phenomena. The indoor heat gain $\dot{Q}_{in}$ induced by the ventilated BIPV wall can be calculated from equation (2) as:

$$\dot{Q}_{in} = \dot{Q}_{cond} + \dot{Q}_{vent} \tag{2}$$

Where $\dot{Q}_{cond}$ is the rate of conductive heat transfer (W) transmitted through the interior wall panels of the ventilated BIPV to the indoor air, and $\dot{Q}_{vent}$ is the heat gain (W) that flowed in through the indoor vent.
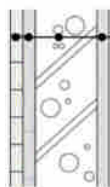
	Tile	Mortar	RC	Mortar
Thickness(mm)	10	15	120	10
Density (kg/m^3)	2400	2000	2200	2000
Specific heat (kJ/kg K)	0.84	0.8	0.88	0.8
Thermal conductivity (W/m K)	1.3	1.5	1.4	1.5

	Al panel	Rock wool	Air	Sodium Calcium plate
Thickness (mm)	6	20	20	25
Density (kg/m^3)	2700	1200	1.6	900
Specific heat (kJ/kg K)	0.9	0.84	0.84	0.63
Thermal conductivity (W/m K)	210	0.051	0.11	0.15

(a) Exterior wall of RC buildings   (b) Exterior wall of light steel houses

Figure 4. Thermal properties of each individual layer of the exterior walls

RESULTS AND DISCUSSION
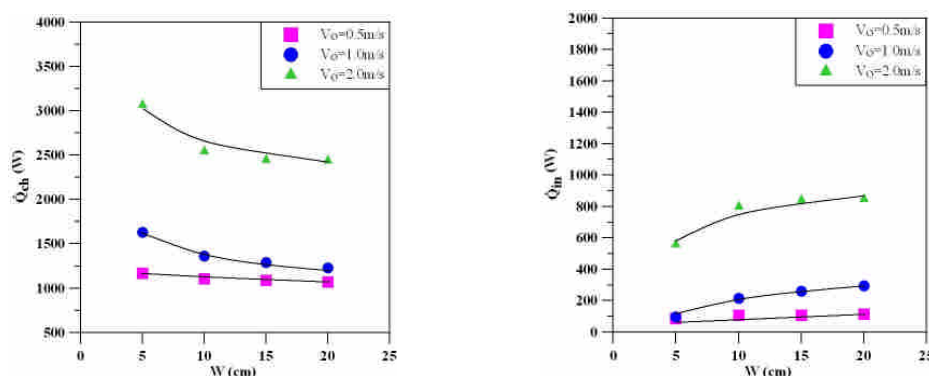
Heat removal rate and indoor heat gain

The CFD simulations were conducted under the conditions of three outdoor wind velocities, four airflow channel widths and six indoor vent heights, as listed in Table 1. Airflow simulations of different airflow channel widths (Vo=0.5 m/s and H=45 cm) are shown in Figures 5. The results showed that when the outdoor airflow entered the inlet of the BIPV wall, part of the airflow would enter indoor through the indoor vent, and part of it would flow upward and out through the top outlet which would also be entrained by the outdoor airflow around the outlet. When the flow channel was widened, besides an upward airflow with a hydraulic jump around the channel lower part, part of the channel airflow would enter the indoor vent in an upward slanting manner, enhancing the indoor vent flow.

(a) W=5 cm	(b) W=10 cm
(c) W=15 cm	(d) W=20 cm
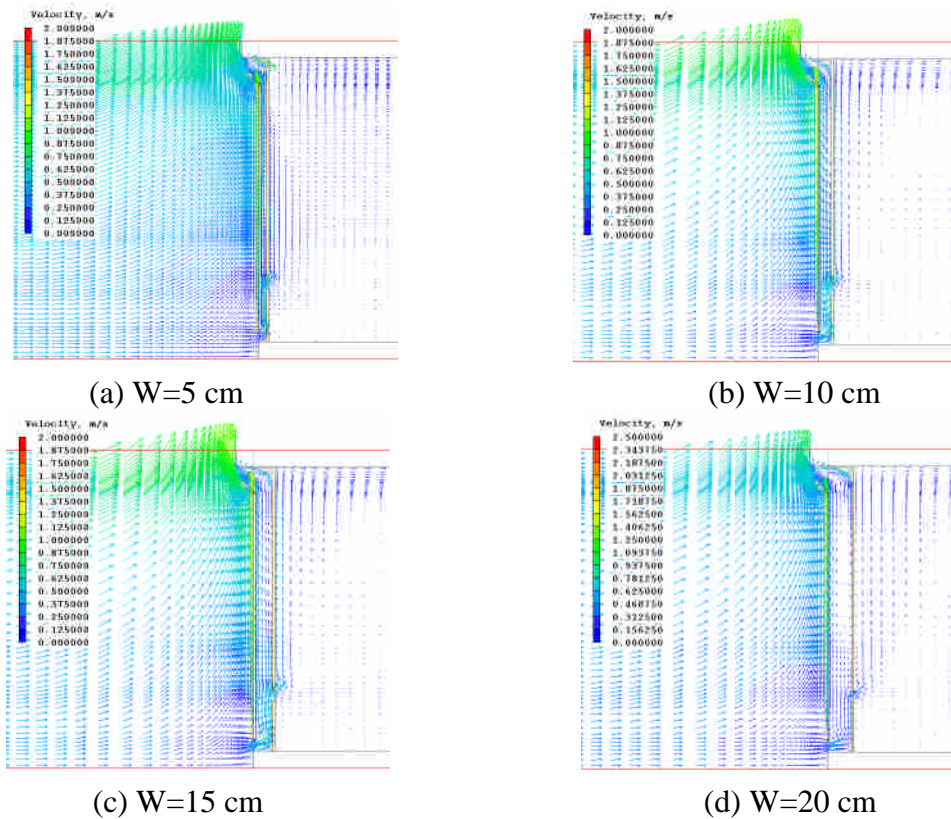
Figure 5. CFD simulations of flow patterns (cases with V_o =0.5 m/s and H=45 cm)

The effects of outdoor wind velocity and channel width on the heat removal rate and indoor heat gain were showed in Figure 6, calculated using equations (1) - (2). A wider the airflow channel results in a lower heat removal rate for the ventilated BIPV wall. When the outdoor wind velocity was 0.5 m/s, the channel width had a minimal effect on the heat removal rate, and its average value was about 1073-1155 W. When the outdoor wind velocity was 1.0 m/s and the channel width was 5 cm, the heat removal rate was found to be at its maximum. A larger channel width results in a lower heat removal rate. An average heat removal rate value of approximately 1228-1628 W was documented. When the outdoor wind velocity was 2.0 m/s, with an airflow channel width greater than 10 cm, the heat removal rate reached an average of 2439-3065 W.

When the outdoor wind velocity was 0.5 m/s, the indoor heat gain of the ventilated BIPV walls was approximately 143-148 W, indicating that the indoor heat gain was not significantly affected by channel width. When the outdoor wind velocity was 1.0 m/s, the indoor heat gain was approximately 98-295 W, indicating that an increase in channel width results in an increase in indoor heat gain. When the outdoor wind velocity was 2.0 m/s, the indoor heat gain value was 558-847 W, indicating that an increase in the airflow channel width increases the indoor heat gain. When the width was greater than 10 cm, the indoor heat gain remained constant. Correlations for predicting the heat removal rate and indoor heat gain by outdoor wind velocity and channel width are $\dot{Q}_{ch} = 2203 V_o W^{-1/5}$ and $\dot{Q}_{in} = 106.5 V_o^{1.4} Ln(W)$, respectively. These equations are valid when the outdoor wind velocity is V_o =0.5-2.0 m/s, the airflow channel width is W =5-20 cm, and the indoor vent height is H=15-90 cm. Details of the correlation development and relevant results can be found in our previous work. (Lai and Lin, 2011) (Lin *et al.*, 2011)


Figure 6. The effects of outdoor wind velocity (Vo) and channel width (W) on the heat removal rate (left) and indoor heat gain (right)

Suggested structure and its performance tests

Construction feasibility and cost (among other considerations) must be considered when developing the experiment prototype described in the previous section into a practical building construction (the ventilated BIPV curtain wall). Herein, the ventilated BIPV curtain wall was established and installed on an existing building as a replacement for the external walls. In addition, thermal performance was tested in accordance with the method described before. Fig. 7 shows the assembly process for the ventilated BIPV curtain wall.

This study suggests that the ventilated BIPV wall can be used to form one kind of metal curtain walls, which replaced metal exterior panels as photovoltaic panels, while aluminum can be left as the back plane in the interior walls to form air flow channels between the front and back materials. A single curtain wall size was 2.26 m (H) x 0.77 m (W), and the exterior walls were formed with two photovoltaic panels mounted on the surrounding aluminum framework. Many holes with 1.5 cm in diameter were drilled on the horizontal aluminum frames (Fig. 7 (a)) for airflow purpose. The airflow inlet and outlet at the upper and lower portions of the curtain wall were composed of 3-mm-thick aluminum punching louvers (Fig. 7 (b)), and the backside was encapsulated with a 3-mm aluminum plate (Fig. 7 (c)). The power line was routed by pulling the line toward the vertical column; it was then directed inside through the curtain wall backside.
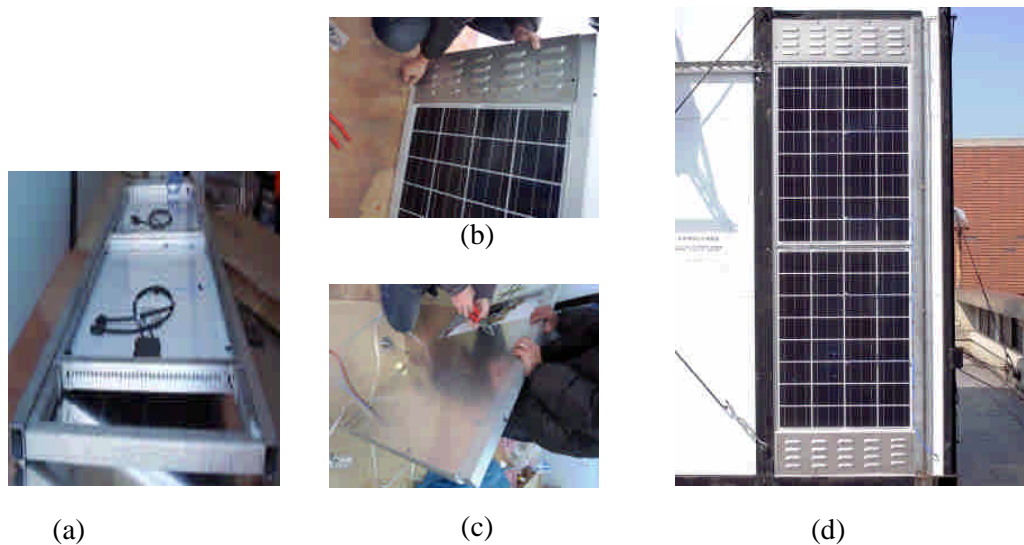
Figure 7. Establishment of the ventilated BIPV curtain wall

CONCLUSION

The CFD simulations of flow patterns and temperature distributions of the ventilated BIPV walls were conducted under the conditions of three outdoor wind velocities, four airflow channel widths and six indoor vent heights. It shows that a wider the airflow channel results in a lower heat removal rate for the ventilated BIPV wall. The heat removal rate and indoor heat gain are not significantly affected by indoor vent height. The effects of outdoor wind velocity and channel width on the heat removal rate and indoor heat gain are introduced.

ACKNOWLEDGEMENTS

REFERENCES

Dubey, S, and Tiwari, G. N. (2009) "Analysis of PV/T flat plate water collectors connected in series." *Solar Energy*, 83, 1485-1498.

Lai, C. M., and Lin, Y.P. (2011) "Energy saving evaluation of the ventilated BIPV walls." *Energies*, 4, 6, 948-959.

Lin, Y.P., Chiang, C. M., and Lai, C. M. (2011) "Energy efficiency and ventilation performance of ventilated BIPV walls." *Engineering Applications of Computational Fluid Mechanics,* 5, 4, 479-486.

Spalding, D.B. (1994) *The PHOENICS encyclopedia*. CHAM Ltd: London, UK.